Analyzing Effects of Solar Variability and System Location on LMP Prices

Mesude Bayrakci-Boz
Penn State Hazleton
Hazleton, PA
mzb187@psu.edu

Joseph Ranalli
Penn State Hazleton
Hazleton, PA
jar339@psu.edu

***Abstract*—Optimal power flow has been solved to show possible effects of solar variability and location of solar systems on electricity price using the IEEE 30 Bus Test system. Different densities of simulated solar generation plants were used, with higher-density plants exhibiting higher variability of generation. The effects of different solar variability conditions tested in this study were found to be minimal on the absolute reduction in local marginal prices (LMPs), but low-density plant distributions exhibited smaller and less frequent fluctuations in the price. In some cases, solar generation was observed to reduce the LMP to zero, resulting from congestion that limited the export of electricity. We observed that lower-density generation distributions could reduce the frequency of these rapid price fluctuations. The location of solar systems within the grid can also have a significant impact on LMPs. When solar generation is installed at a high demand bus, the LMP typically decreased at both the local and neighboring buses. When the solar systems are installed at a low demand bus, the LMPs were observed to increase or decrease depending on the demand and congestion. This work highlights the importance of the effects of solar system location on LMP.**

***Index Terms*—solar, photovoltaics, variability, spatial aggregation, wavelet variability model, locational marginal price, LMP, demand**

I. Introduction

Renewable energy generation, including solar photovoltaics (PV), naturally exhibits a higher degree of variability than traditional sources of generation and is naturally spatially distributed throughout the generation environment. The distributed nature of PV generation poses technical and economic challenges that must be overcome to enable higher levels of renewable penetration onto the electrical grid. Besides technical challenges, it is important to understand the role that distributed solar PV may play in driving electricity prices in the marketplace. Both solar variability and distribution may be expected to play a role in determining the electricity price.

An important electricity metric in the energy market is hourly wholesale price, known as the Locational Marginal Price (LMP). LMP is the marginal cost of transferring an incremental unit of energy from one network location to another location in the network. The price can change according to the balance between supply and demand, and congestion. A review of literature shows numerous studies conducted to analyze the effect of solar systems on LMP. For example, Schwabe et al. [1] made a comparison among average prices of electricity based on the combination of empirically derived energy generation from two photovoltaic systems and LMPs for two regions. Hemmati et al. demonstrated the impacts of renewable energy on flow-gate marginal pricing and LMPs using an IEEE six bus test system [2]. Albadi et al. created two scenarios; one large solar project and small geographically dispersed solar projects in Oman, and investigated the implications on transmission losses and LMPs [3]. Mohammad et al. considered the social welfare maximization problem of Independent System Operators (ISOs), and proposed a new decomposition for LMP after analyzing the effect of renewable energy systems on LMPs [4]. Jin et al. [5] created a model of LMP-based partition optimal economic dispatch with wind and photovoltaic systems that provide 42% of the total generation capacity of the test system.

However, existing studies did not account for the effects of how the distribution of generation with respect to solar variability impacts electricity pricing. This study analyzes these effects on electricity pricing by solving optimal power flow with MATPOWER for the IEEE 30 Bus Test Case. LMPs were obtained for solar systems connected to the grid considering two different generation distribution density (i.e. variability) conditions. Then, we evaluated how the solar system deployment density and its location within the test bus affects the LMPs.

II. Methodology

A. Variability Modeling

A major component of the variability inherent to solar generation is induced by cloud motion across a distributed generation facility [6]. Previous studies have described the inverse relationship between the density of the generation plant's spatial distribution and the variability of the output: that is, generation spread over a smaller spatial extent exhibits a higher degree of variability than generation spread out over a broader geographic area [7]. As variability of generation may be expected to drive short term electricity prices, we may expect that high- and low-density distribution of generation will have differing impacts on the electricity price.

A region representing a single node of the IEEE network model was approximated as covering a geographic range of 10 km x 10 km. A total of 30 MW of generation were modeled as a generator, feeding into the node. Two different generation cases were considered: one large 30 MW plant and one

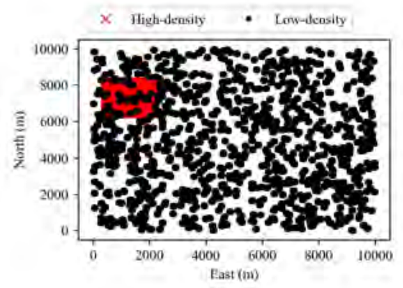

Fig. 1. Sample plant layout. In both cases, 21 MW of total rated capacity are modeled.

TABLE I
VARIABILITY METRICS FOR 2019 REF. DAYS FROM SURFRAD - PSU

Category	Date	Day of Yr	Mean k_c	VS	VI	DARR
Clear	Mar 23	082	1.07	0.07	1.20	214.7
Clear	Mar 26	085	1.11	0.07	1.04	179.2
Cloudy	Mar 01	060	0.31	0.04	1.06	152.2
Cloudy	Mar 21	080	0.16	0.04	1.03	161.9
Variable	Apr 20	110	0.88	1.45	21.46	5706.4
Variable	Jun 14	165	0.86	2.13	30.03	8093.5

thousand small 30 kW plants. A spatial density of 41 MW per acre was used to determine the geographic size of these plants. Thus, the 30 MW plant resulted in a high-density concentrated generation facility, while the 1000 smaller plants resulted in a low-density distribution within the overall area. The plants were randomly centered within the given geographic area and built out to the necessary size to match the capacity scale desired. A sample random layout is in Fig. 1.

In order to model the differences in spatiotemporal variability between the loosely- and densely-distributed PV generation, we utilized the Wavelet Variability Model (WVM) [8] as implemented in PVLIB Python [9]. The WVM represents how the variability in the irradiance time series measured at a single point is smoothed out due to a spatially distributed plant. It does so via selective reduction in the magnitude of wavelet mode amplitudes as a function of wavelet timescale. Short timescales (higher frequencies) are reduced the most, while longer (low frequency) timescales retain their amplitude. The degree to which each wavelet mode's amplitude is scaled down is determined by the modeled time series correlation between spatially disparate portions of the site; a greater spatial separation leads to more significant smoothing of the time series.

We used individual days from the SURFRAD database [10] as representative reference global horizontal irradiance (GHI) time series. These reference (i.e. point measurement) time series were taken for the SURFRAD site *PSU*, located in central Pennsylvania. Data were considered for the entire year of 2019, and several representative clear, cloudy and variable days were manually identified and were compared on the basis of common variability metrics [11]: Variability Score (VS) [12], Variability Index (VI) [13] and Daily Aggregate Ramp Rate (DARR) [14]. In the case of all of these metrics, a higher value corresponds to more variability. Values for these metrics for the reference days considered are given in Table I. As is evident, both clear and cloudy days exhibited low values of the variability as compared to the variable days. While the level of variability between the clear and cloudy days was similarly low, they are differentiated by the cloudy days exhibiting a much lower mean value clear-sky index (k_c).

In order to compute the simulated electricity generation from the high- and low-density distributed plants, the irradiance time series were used as an input measurement to the WVM, which provides a prediction of the smoothed irradiance over the aggregate plant. The output of the low-density plant would be expected to have lower variability (smoother time series) than the high-density plant modeled in this study. Comparisons of high- and low-density plant irradiance time series are shown in Fig. 2. It is evident that the low-density plant case exhibits reduced magnitude of fluctuations in the irradiance. The frequency dependence of the variability reduction can be seen by considering the magnitude of transfer function for each case relative to the input, as shown in Fig. 3.

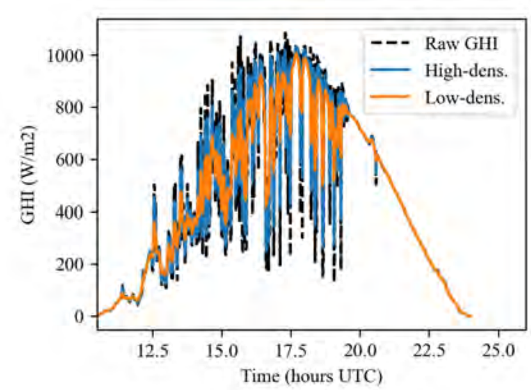

Fig. 2. Sample WVM output time series smoothed by the two different plant layouts for a variable day, Apr 20, 2019. Input in each case is a 1 minute resolution time series from SURFRAD.

As this model represents a hypothetical plant and we are principally concerned with how differences in the variability affect the electricity price, we represented the relationship between irradiance and plant electrical output as a simple scaling operation. Aggregate irradiance time series from the WVM were normalized such that a computed irradiance of 1000 W/m^2 was assumed to produce electrical power at the rated capacity (30 MW) of the overall plant, as specified in Section II-A.

B. Optimization

The effects of solar variability and location of solar systems on electric prices were investigated through solving optimal power flow (OPF) using the IEEE 30 Bus Test in MATPOWER, an open source MATLAB simulation package [15].

OPF determines the best operating levels of the generators at the lowest cost, considering any operational limits of

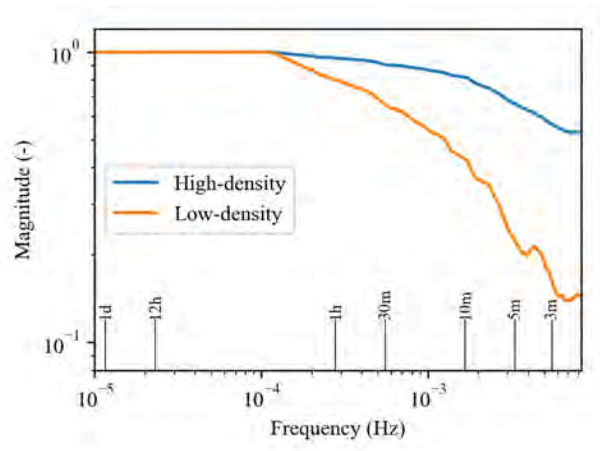

Fig. 3. Sample WVM output transfer functions for the two plant distributions demonstrating the frequency dependence of the variability reduction for a variable day, Apr 20, 2019. Several common timescales are labeled on the frequency axis.

generation and transmission facilities. The process of OPF is:

$$min[f(x)] \tag{1}$$

Subject to the following conditions:

$$g(x) = 0 \tag{2}$$

$$h(x) \leq 0 \tag{3}$$

$$x_{min} \leq x \leq x_{max} \tag{4}$$

The objective function $f(x)$ consists of the polynomial cost of generator injections. The equality constraints $g(x)$ are the real and reactive power balance equations. The inequality constraints $h(x)$ consist of two sets of n_l branch flow limits as nonlinear functions of the bus voltage angles and magnitudes, one for the *from* end and one for the *to* end of each branch.The variable limits x_{min} and x_{max} include an equality constraint on any reference bus angle and upper and lower limits on all bus voltage magnitudes and real and reactive generator injections [16].

The IEEE 30 Bus Test Case, from December, 1961, represents data collected in the Midwestern US by the American Electric Power System [17]. The MATPOPWER package has the IEEE 30 bus test case with some modifications: the data was taken from Alsac et al. [18] with branch parameters rounded to the nearest 0.01, shunt values divided by 100, and the shunt on bus 10 moved to bus 5, with the load at bus 5 zeroed out. Generator locations, costs and limits and bus areas were taken from Ferrero at al. [19]. Generator Q limits were derived from [18], using their Pmax capacities. V limits and line limits were taken from [18]. The IEEE 30 case is shown with line limits, demand for each bus and generators in Figure 4.

The OPF was first run for the IEEE 30 bus system without any solar systems to create a LMP baseline. Then, solar systems were added to the system as a generator for each

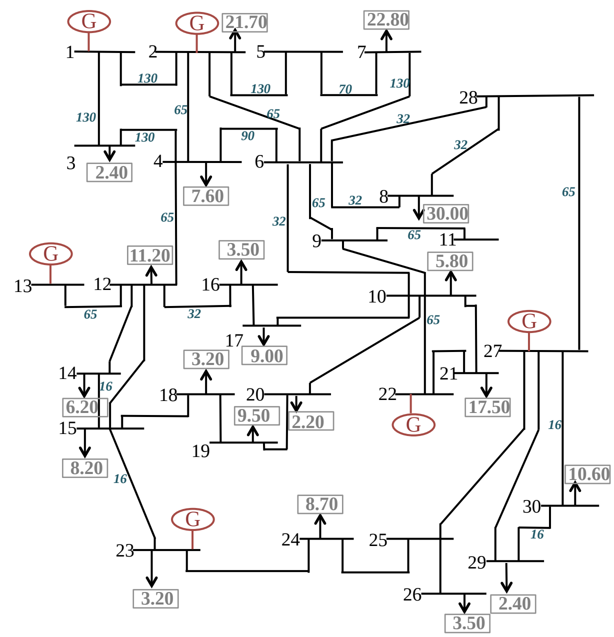

Fig. 4. IEEE 30 bus system test case. The red G in the circle shows the generators, while the grey numbers in the rectangle show the demand values, and the dark blue numbers show the line limits

TABLE II
SOLAR TEST BUS PLACEMENT DETAILS

Bus Number	Demand (MW)	Neighbour Buses
20	2.2	Bus 10, Bus 19
29	2.4	Bus 27, Bus 30
14	6.2	Bus 12, Bus 15
30	10.6	Bus 27, Bus 29
8	30	Bus 6, Bus 28

of the clear, cloudy, and variable days considering high- and low-density plant distribution scenarios. The OPF was run accordingly for each scenario. Bus demand was considered when choosing which buses to add the PV systems to. Five buses were chosen to represent different levels of demand. These five buses and the associated demand for each bus are shown in Table II. LMPs at these five buses and their neighbor buses were obtained and analyzed for each scenario.

The results were compiled on a comparative basis, relative to the baseline LMP with no solar generation. In order to do this, a percent difference range was determined for each five buses, based on the LMPs with- and without- a solar system. Equation 5 was used for this calculation.

$$LMP_{diff}(\%) = \left(\left(\frac{LMP_{with}}{LMP_{without}} \right) - 1 \right) \times 100\% \tag{5}$$

For all these scenarios, the variables in MATPOWER were modified to include real power generation (Pg), imaginary power generation (Qg), max real power (Pmax), min real power (Pmin), max imaginary power (Qmax), min imaginary power (Qmin), and generation costs.

It was assumed that PV systems produce power proportional to irradiance, based upon their rated capacities, as stated previously. The minimum real power value for PV systems was assumed to be zero. PV systems do not produce reactive power, but inverters may be used for this purpose. In the literature, the maximum reactive power has been assumed to be 1/3 of maximum real power [20] and minimum reactive power is the negative of the maximum reactive power value. These assumptions were also used in this study. Finally, the generation costs for the PV systems were set to zero since those would be paid from the initial cost of the PV systems, with no ongoing fuel costs.

III. Results and Discussion

The 30 MW solar system was first placed at bus 29 and LMP changes at this bus were analyzed with high- and low-density generation distributions for the three different days (clear, cloudy, and variable). The total generation on the bus for these days is around 190 MW. With 30 MW rated capacity from PV systems, this results in PV penetration of around 15%. On a clear day, March 26, the LMP price at bus 29 was \$3.96/MWh for the base case scenario (i.e. no solar system) and decreased to a range of \$3.94/MWh to \$3.34/MWh when high-density solar case was added, as shown in Figure 5a. Similar results were observed for the low-density case as well. This translates into a 1 to 15% overall decrease in the range of LMPs for low- and high-density cases. On a cloudy day, March 21, the LMP decrease was very small regardless of the solar generation density, a decrease corresponding a range from 1 to 1.9%, as seen in Figure 5b. The results indicate that there is no significant difference between the high- and low-density solar cases analyzed in this study during clear and cloudy days. This makes sense, as the relatively low variability of these days leads to only small differences caused by the distribution of solar generation.

However, a different pattern of LMP changes is observed during a variable day, June 14. The LMP exhibits significant differences between the high- and low-density cases, as in Figure 5c. Overall, there is a pattern of solar causing a slight reduction in the LMP. However, multiple times the LMP fluctuates from the reduced value to zero and back in a very short time span. We attribute this to congestion on enough neighboring lines to result in no pathway for the electricity to be exported, and thus a price of zero is reached. These zero-price conditions occur rapidly, and repeatedly, and are observed more often for the high-density distribution of solar. The LMP values become zero for approximately 114 minutes of the day (8%) and 45 minutes (3%) for high- and low-density distributions, respectively. In addition, even when LMP is not zero, it experiences a higher degree of fluctuation than that seen in the low-density distribution case. This shows that accounting for the effect of solar distribution (variable day scenario) on LMPs is very important, since these sudden changes of price may give market participants misleading price signals. The low-density distribution of solar reduces the risk of these sudden changes in price and mitigates the price risk.

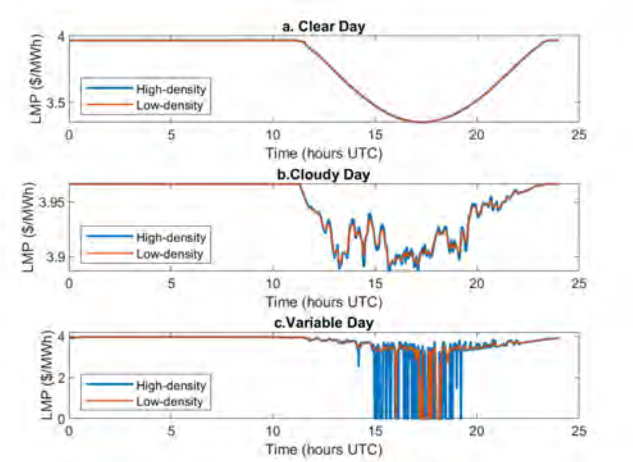

Fig. 5. LMPs at bus 29 in a clear, cloudy and variable day when solar system is placed at bus 29.

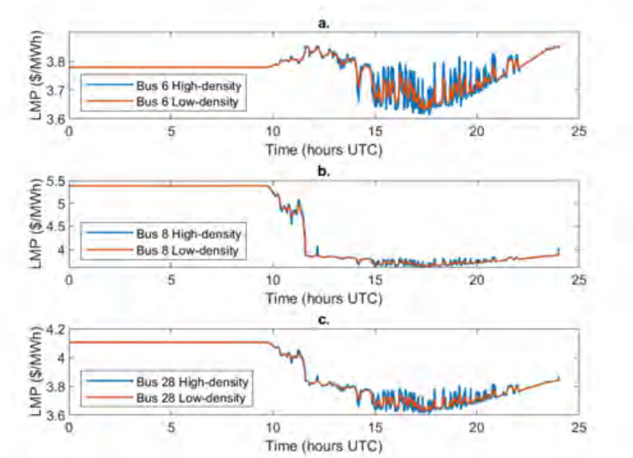

Fig. 6. Variable day LMPs at bus 6, 8, and 28 when solar system is placed at bus 8 with high-density and low-density.

In order to further investigate how LMP changes at neighboring buses to the solar system, we analyzed high- and low-density distribution plants on a variable day for each of the bus cases presented in Table II. The results are shown in Figures 6 to 10. Overall, LMP decreases at most buses for both low- and high-density distributions with a relatively lower minimum price in the high-density case. However, the price experiences a lower degree of fluctuation for the low-density case. This is consistent with the lower variability of the low-density case due to additional smoothing of the time series.

The amount of decrease in price at the bus where solar system is placed is greater than the decrease seen for the neighboring buses. This is because the solar generation would be used first by the local bus, with the surplus sent to other buses. For example, demand at bus 14 (Fig. 7) is 6.20 MW and all the demand can be supplied from the solar system, such that some is exported to neighboring buses. In this case, the LMP

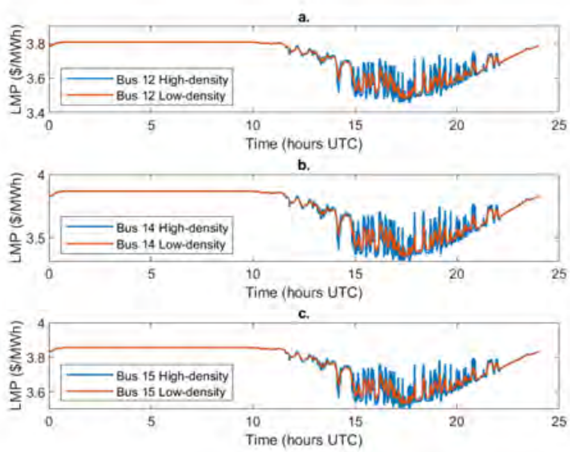

Fig. 7. Variable day LMPs at bus 12, 14, and 15 when solar system is placed at bus 14 with high-density and low-density.

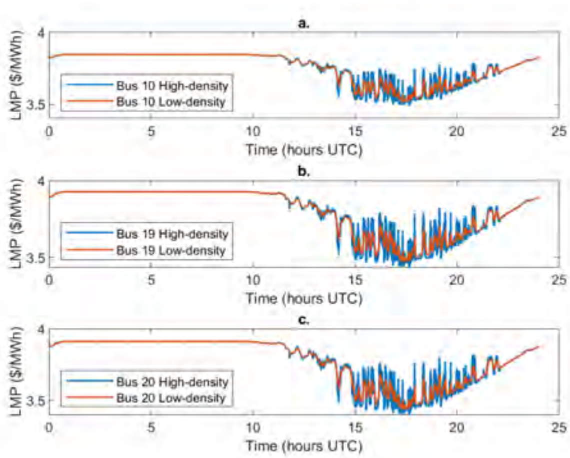

Fig. 8. Variable day LMPs at bus 10, 19, and 20 when solar system is placed at bus 20 with high-density and low-density.

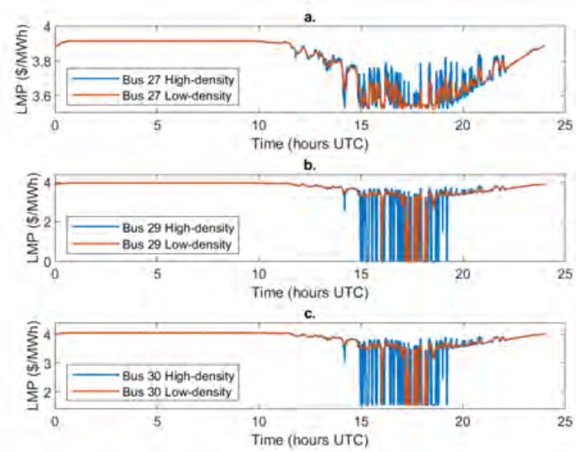

Fig. 9. Variable day LMPs at bus 27, 29, and 30 when solar system is placed at bus 29 with high-density and low-density.

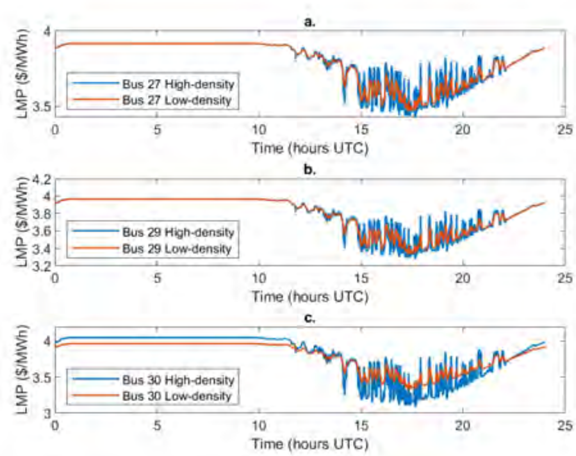

Fig. 10. Variable day LMPs at bus 27, 29, and 30 when solar system is placed at bus 30 with high-density and low-density.

decreases around 14% for bus 14 and 9% for buses 12 and 15. All the LMPs percent changes from maximum decrease to maximum increase for each case is tabulated in Table III. Negative numbers indicate a decrease in LMPs, while positive numbers an increase. Placing a solar system in the IEEE test case results in LMP decrease from 3% to 100% depending on the buses.

While installation of solar systems generally results in a reduction in LMP on neighboring buses, it can be seen that LMP may increase with solar system penetration at some buses in other parts of the grid. For example, when the solar system was added to bus 20, the LMP decreases around 13% for bus 20 with respect to the base case, but increases around 7% for bus 8, as seen in Figure 11. The demand for bus 20 is 2.2 MW and the solar system produces much more than this demand. Thus, the rest of the energy produced is sent to other buses. This causes congestion on the line between bus 6 and bus 8, which leads to higher LMP at bus 8. The results indicate how LMPs change with respect to where solar systems are placed alongside the demand conditions and further investigation is needed to analyze the effect of solar generation on congestion with different cases.

IV. Conclusion

Solar generation has an impact on LMPs, and the extent of this impact is affected by many factors. In this study, the effects of solar generation distribution density (and concurrently variability of generation) and bus location of solar systems on LMPs were investigated. This objective was achieved by solving the optimal power flow using the IEEE 30 Bus Test system in MATPOWER. The results show the effects of different solar variability conditions tested in this study are similar on LMPs during clear and cloudy days. However, solar distribution density (i.e. variability) has significant effect on

TABLE III

MAXIMUM LMP PERCENT INCREASE OR DECREASE(%) FOR EACH BUS LOCATION AND NEIGHBORS.

		Bus 6		Bus 8		Bus 28	
		Max. ↓	Max. ↑	Max. ↓	Max. ↑	Max. ↓	Max. ↑
Solar System at Bus 8	High Density	-4.410	1.989	-32.971	0.049	-12.088	0.011
	Low Density	-3.881	1.993	-32.571	0.048	-11.619	0.011
		Bus 12		Bus 14		Bus 15	
		Max. ↓	Max. ↑	Max. ↓	Max. ↑	Max. ↓	Max. ↑
Solar System at Bus 14	High Density	-9.329	0.001	-14.414	0.002	-9.222	0.001
	Low Density	-8.596	0.001	-13.372	0.001	-8.504	0.001
		Bus 10		Bus 19		Bus 20	
		Max. ↓	Max. ↑	Max. ↓	Max. ↑	Max. ↓	Max. ↑
Solar System at Bus 20	High Density	-9.263	0.003	-12.567	0.001	-13.135	0.002
	Low Density	-8.532	0.004	-11.628	0.001	-12.160	0.002
		Bus 27		Bus 29		Bus 30	
		Max. ↓	Max. ↑	Max. ↓	Max. ↑	Max. ↓	Max. ↑
Solar System at Bus 29	High Density	-10.098	0.000	-100.000	0.000	-61.842	0.001
	Low Density	-10.092	0.000	-100.000	0.000	-61.842	0.001
		Bus 27		Bus 29		Bus 30	
		Max. ↓	Max. ↑	Max. ↓	Max. ↑	Max. ↓	Max. ↑
Solar System at Bus 30	High Density	-12.507	0.000	-17.289	0.000	-23.755	0.001
	Low Density	-11.466	0.000	-15.879	0.000	-17.631	-2.084

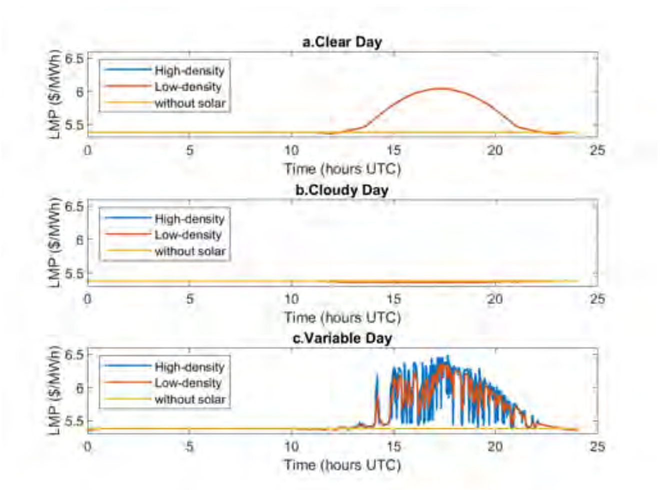

Fig. 11. LMPs at bus 8 when solar system is placed at bus 20 with high-density and low-density in a clear, cloudy and variable day.

LMPs during a variable day. The results also show that the LMP decreases for the buses in which the solar system is added and for the neighbour buses.Such decrease ranges from 3% to 100%. Cases with 100% reduction appear to result from high levels of congestion preventing the export of power. It was observed that low-density solar plant distributions reduce the occurrence of these zero-price conditions by smoothing out the variability in the generation time series.

It was also observed that when a solar system is added to a low demand bus (e.g. bus 20), the LMP decreased for the low demand bus, but it increased for high demand buses (e.g.bus 8). This results from the local surplus solar generation being sent to other buses, which can result in congestion and thus, increase in LMP. This clearly indicates the effects of solar system location on LMPs. The results from this study can be used for informed planning and decision-making process for solar system installation. Additional work is needed to further investigate the effects of solar variability on LMPs by more comprehensively placing solar system at each bus, considering a more complete set of daily irradiance conditions days and varying solar penetration levels.

REFERENCES

[1] U. Schwabe and P. Jansson, "Utility-interconnected photovoltaic systems reaching grid parity in new jersey," in *IEEE PES General Meeting*, 2010, pp. 1–5.

[2] R. Hemmati and R.-A. Hooshmand, "Impacts of renewable energy resources and energy storage systems on the flow-gate prices under deregulated environment," *Journal of Renewable and Sustainable Energy*, vol. 9, no. 3, p. 035502, 2017. [Online]. Available: https://doi.org/10.1063/1.4984622

[3] M. H. Albadi, Y. M. El-Rayani, E. F. El-Saadany, and H. A. Al-Riyami, "Impact of solar power projects on lmp and transmission losses in oman," *Sustainable Energy Technologies and Assessments*, vol. 27, pp. 141–149, 2018. [Online]. Available: https://www.sciencedirect.com/science/article/pii/S221313881730262X

[4] M. J. Poursalimi Jaghargh and H. R. Mashhadi, "An analytical approach to estimate structural and behavioral impact of renewable energy power plants on lmp," *Renewable Energy*, vol. 163, pp. 1012–1022, 2021. [Online]. Available: https://www.sciencedirect.com/science/article/pii/S0960148120313343

[5] H. Jin, Y. Teng, T. Zhang, Z. Wang, and B. Deng, "A locational marginal price-based partition optimal economic dispatch model of multi-energy systems," *Frontiers in Energy Research*, vol. 9, 2021. [Online]. Available: https://www.frontiersin.org/article/10.3389/fenrg.2021.694983

[6] T. E. Hoff and R. Perez, "Quantifying PV power Output Variability," *Solar Energy*, vol. 84, no. 10, pp. 1782–1793, Oct. 2010. [Online]. Available: http://www.sciencedirect.com/science/article/pii/S0038092X10002380

[7] J. Marcos, L. Marroyo, E. Lorenzo, and M. García, "Smoothing of PV power fluctuations by geographical dispersion," *Progress in Photovoltaics: Research and Applications*, vol. 20, no. 2, pp. 226–237, 2012. [Online]. Available: https://onlinelibrary.wiley.com/doi/abs/10.1002/pip.1127

[8] M. Lave, J. Kleissl, and J. S. Stein, “A Wavelet-Based Variability Model (WVM) for Solar PV Power Plants,” *IEEE Transactions on Sustainable Energy*, vol. 4, no. 2, pp. 501–509, Apr. 2013.

[9] W. Holmgren, C. Hansen, and M. Mikofski, “pvlib python: a python package for modeling solar energy systems,” *Journal of Open Source Software*, vol. 3, no. 29, p. 884, Sep. 2018. [Online]. Available: https://joss.theoj.org/papers/10.21105/joss.00884

[10] J. A. Augustine, J. J. DeLuisi, and C. N. Long, “SURFRAD–A National Surface Radiation Budget Network for Atmospheric Research,” *Bulletin of the American Meteorological Society*, vol. 81, no. 10, pp. 2341–2358, Oct. 2000, publisher: American Meteorological Society Section: Bulletin of the American Meteorological Society.

[11] G. M. Lohmann, “Irradiance Variability Quantification and Small-Scale Averaging in Space and Time: A Short Review,” *Atmosphere*, vol. 9, no. 7, p. 264, Jul. 2018. [Online]. Available: https://doaj.org

[12] M. Lave, M. J. Reno, and R. J. Broderick, “Characterizing local high-frequency solar variability and its impact to distribution studies,” *Solar Energy*, vol. 118, pp. 327–337, 2015.

[13] J. S. Stein, C. W. Hansen, and M. J. Reno, “The Variability Index: A New and Novel Metric for Quantifying Irradiance and PV Output Variability,” in *Proceedings of the World Renewable Energy Forum*, Denver, CO, May 2012, pp. 13–17.

[14] R. van Haaren, M. Morjaria, and V. Fthenakis, “Empirical assessment of short-term variability from utility-scale solar PV plants,” *Progress in Photovoltaics: Research and Applications*, vol. 22, no. 5, pp. 548–559, 2014, _eprint: https://onlinelibrary.wiley.com/doi/pdf/10.1002/pip.2302. [Online]. Available: https://onlinelibrary.wiley.com/doi/abs/10.1002/pip.2302

[15] R. D. Zimmerman and C. E. M.-S. . M. V. . S. A. https://matpower.org.

[16] R. D. Zimmerman and C. E. Murillo-Sanchez, “Matpower user’s manual, version 7.1. 2020.”

[17] C.-H. Lo and N. Ansari, “Alleviating solar energy congestion in the distribution grid via smart metering communications,” *IEEE Transactions on Parallel and Distributed Systems*, vol. 23, no. 9, pp. 1607–1620, 2012.

[18] O. Alsac and B. Stott, “Optimal load flow with steady-state security,” *IEEE Transactions on Power Apparatus and Systems*, vol. PAS-93, no. 3, pp. 745–751, 1974.

[19] R. Ferrero, S. Shahidehpour, and V. Ramesh, “Transaction analysis in deregulated power systems using game theory,” *IEEE Transactions on Power Systems*, vol. 12, no. 3, pp. 1340–1347, 1997.